Journal of Hydroscience and Hydraulic Engineering
Vol. 17, No.1 May, 1999, 87-101

FLOW RESISTANCE IN AN OPEN CHANNEL WITH AN ALTERNATIVE RIFFLE-POOL ARRANGEMENT

By

K.Michioku[1], O.Takemoto[2] and M.Hirota[2]

1) Dept. Architecture and Civil Engineering, Kobe University
1-1 Rokkodai, Nada, Kobe 657-8501, JAPAN
2) Civil Engineering Bureau, Hyogo Prefecture Government
Shimoyamate-dohri, Chuo, Kobe 650, JAPAN

SYNOPSIS

For creation of a natural river environment, a channel restoration producing variety of flow fields is much appreciated in recent years. A typical way of such works is arranging structures such as riffles, pools, islands, and vegetation along a river course. After restoration works attentions should be paid on ecological or environmental changes in a river system. Additionally, flow resistance has to be carefully evaluated for prevention of flood disasters, because this type of river works absolutely increases channel's roughness.

The present study deals with flow hydrodynamics in open channels in which riffles and pools are alternately and regularly arranged along a flume. In laboratory experiments, measurements were made with respect to flow resistance, water surface profiles and velocity vectors. A drag force coefficient was experimentally formulated as a function of geometrical parameters of the riffle-pool model. This was applied to a one-dimensional analysis for evaluation of flow resistance. The friction coefficient computed by the method was well correlated with the experimental data.

The present study helps us in designing river channel structures from a hydrodynamic point of view. It should be kept in mind that only the creation of a nature-friendly river ecosystem is sometimes dangerous; the restored channel should function as a flow conveyer of high performance flood.

INTRODUCTION

In recent years, so-called "near-nature river works" are extensively applied in many river systems. The basic idea is to create nature-friendly flow fields and to recover original ecosystems that used to be widely inhabited. The objective of this restoration project is not only recovery of the original nature but also protection of river channels from storm waters.

In most this type of restoration works, however, channel roughness is certainly increased, because structures such as islands, riffles, bars, pools, rocks and vegetation are installed along a channel section. Therefore, it is desperately necessary to discuss if the restored channel would function for flood disaster prevention.

In the present study, extra flow resistance due to riffle-pool

arrangement is experimentally examined. The situations that can be examined are, however, rather limited, because there could be too many design options of channel geometry. A system considered here is a very simplified one such that a trapezoidal riffle element is alternately arranged along a channel to produce a combination of rapid and slow flow regimes.

In a laboratory experiment, flow velocity is measured to examine hydrodynamics involved in flow resistance increment. A water level measurement is also made to obtain flow resistance. The experimental relationship is applied for a one-dimensional flow resistance modeling.

Finally, it is shown how the study should be extended in aiming at designing a river channel course.

PREVIOUS RESEARCH WORKS

In the present system, we assume a flooded river flowing over a series of riffles and pools. The idea is to reproduce rapid and slow flow regimes. For convenience of parameterization, a set of riffle and pool model is installed regularly and alternately in the longitudinal direction. This is a situation analogous to a compound channel with a meandering main channel and a straight channel with single-row alternate bars. Despite so many researches have been done in these fields, topics of this review should be limited to a compound channel system consisting of straight levee and meandering main channel.

An engineering interest is to evaluate a channel conveyance. James and Wark (7) performed a measurement in a compound meandering channel with varying parameters like sinuosity and flow conditions. Because parameters were limited within small ranges, further experiments are still extensively running by many British researchers on a program from the UK-Flood Channel Facility (UK-FCF). Ervine et al. (1) investigated factors affecting channel conveyance. Their examination was on momentum exchange between flood plain and main channel, channel roughness effects, geometric shape losses and so on. The momentum exchange produces additional flow resistance through internal shear stress, which many researchers have been interested in. This stress component can be separately evaluated by examination of a straight compound channel, which was analyzed by and Fukuoka and Fujita (2) for instance. Recently, more attention is paid on internal flow properties being responsible in increasing flow resistance. A three-dimensional measurement of flow velocity enables us to investigate relationships between velocity fields and flow resistance. Fukuoka et al. (3) carried out a detailed velocity measurement and proposed a conceptual model to show how plunging flows from flood plain to main channel modifies secondary flow cells and so on. Rameshwaren and Willets (9) discussed dependency of energy loss on parameters such as main channel sinuosity, flood plain roughness, etc.. Inshigaki et al. (6) focused their attention the relative depth of main channel to flood plain that predominantly influences flow profiles and wall shear stress.

One of the important findings from many velocity measurements is that the compound meandering channel has totally different flow structures from meandering channels of single cross section. This is a very essential factor in dealing especially with sedimentation and erosion around embankments and levees. Whiting and Deitrich (12) and Rahman et al. (10) carried out experiments in compound meandering flumes with movable bed in order to show how sinuosity or meander wave length affects sand bars development and bank erosion process. Utami and Ueno (11) performed an aircraft measurement of flood flow in a compound meandering section of Tone

River. They discussed a relationship between flow field and sedimentation.

A high-performance numerical scheme could be a powerful tool in describing three-dimensional flow structure. Based on many achievements from experimental works, Jin el al. (8) and Fukuoka and Watanabe (4) succeeded in developing numerical models. The former is a depth averaged two-dimensional model and the latter is a three-dimensional model.

In many of these works, focus has been mainly placed on the flow kinematics rather than flow dynamics. It is expected that further research works will be performed with regard to flow resistance and channel conveyance.

A MODEL SYSTEM

In many river works, a channel is restored in a way that (1) flow consists of rapid and slow streams, (2) there are sudden changes in water depth and (3) a perimeter lining consists of rough and smooth surfaces. The shallower region like flood plains and riffles is very possibly rougher than the deeper region because it is sometimes densely vegetated, armored with large pebbles, installed with artificial structures, etc.. In order to study this situation a channel model is considered as shown in Fig.1, where a coordinate system is defined.

A riffle-pool model is alternately and regularly installed with a streamwise interval λ. The riffle element, which has referred as "flood plain", is a trapezoidal plane with an acute angle of θ in the streamwise direction and with a width of b' in the transverse direction. On the riffle's surface, gravel sands are paved to produce roughness such as vegetation. In this model all of the three factors in a restored channel, i.e. horizontal variations in fluid velocity, water depth and perimeter roughness, are taken into consideration. The system is analogous to a single-row alternative bar system, where a bar is vegetated.

EXPERIMENTAL PROCEDURES

Experimental Arrangement

The model flume is a smooth-walled open channel with dimensions of a 700cm long, 45cm wide and 20cm deep. The experiment is carried out under subcritical uniform flow conditions. By using an electromagnetic velocimeter, two-dimensional velocity vectors are measured with 0.1sec sampling interval for 60sec recording duration.

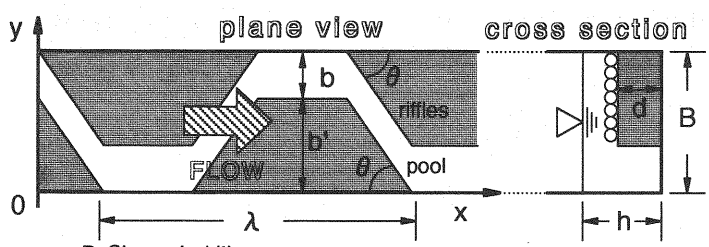

Fig.1 A schematic illustration of the model flume.

A water surface gradient is needed in order to compute flow resistance from a one-dimensional momentum balance. This is obtained by making a point-gauge measurement of water level at several different points. In several cases more detailed measurements are performed to investigate a relationship between a water surface profile and a channel bed profile.

Experimental Conditions

A dimension analysis suggests that a friction coefficient $f \equiv 8gRI/U^2$ is dependent on the following eight parameters,

$$f = \mathrm{Func.}\left(\frac{R}{\lambda}, \theta, \frac{d}{R}, \frac{R}{B}, \frac{R}{b}, \frac{k_S}{h}, \mathrm{Re}, \mathrm{Fr}\right) \tag{1}$$

where, $\mathrm{Re} \equiv UR/\nu$: Reynolds number, $\mathrm{Fr} \equiv U/\sqrt{gD}$: Froude number, $R \equiv \{Bh - d(B-b)\}/(B+2h)$: hydraulic radius, $D \equiv A/B$: hydraulic depth, k_S: equivalent roughness height of the sand-paved flood plain. The other variables should be referred to Fig.1.

In the experiment the width dimensions B and b are fixed to be B=45cm and b=15cm. R and the riffle element's height d are not varied in the "Series-S" and "Series-R", respectively (discussed later). Additionally, the specific equivalent height of roughness k_S/h is set to be constant. After all, three of the dimensionless parameters are excluded from Eq.(1) as

$$f = \mathrm{Func.}\left(\frac{R}{\lambda}, \theta, \frac{d}{R}, \mathrm{Re}, \mathrm{Fr}\right) \tag{2}$$

Experimental conditions are shown in Tables 1 and 2. Two types of experiments are carried out as follows.

Experiment for velocity measurement (Series-V: Table-1)

In order to investigate flow properties involved in drag force generation, 2-D velocity components are measured by using an electromagnetic flow meter. Because of the probe's size and mechanism, it is difficult to measure velocity in a water depth less than 2cm. Then, flow condition in this series is limited to be R=3.6cm and Re≒7,500. Five runs are carried out as listed in Table-1.

Flow resistance measurement (Series-S and R: Table-2)

The following three types of channels are investigated.

(a) A riffle-pool system whose perimeter consists of smooth-walled plates; this is referred as "Series-S".

(b) A system composed of sand-paved riffles and smooth-walled pools, where the channel dimension is exactly same to the Series-S; this is referred as "Series-R".

(c) A straight channel with a compound cross-section whose hydraulic radius is same to the riffle-pool systems in (a) and (b); their case numbers are S-1 and R-7 in Table-2, respectively.

The riffle's surface in the Series-R is made of sand particles with 2 to 4.75mm in diameter paved on a plastic plate. An equivalent roughness height is measured to be k_S=2.77mm.

A detailed point-gauge measurement of water level is made in Cases S-3, 5, 6, 7 and 8 in order to examine an interrelation between a water surface profile and a riffle-pool structure.

VELOCITY FIELDS

Two-dimensional Velocity Profile

In Fig.2 velocity vectors in a x-y horizontal plane of z=3.8cm are shown for the five different cases. The thick line represents the riffle-pool arrangement.

Through comparison of V-1, V-2 and V-3, one can see effects of the angle θ on velocity fields. Here, V-3 is investigated from a scientific interest to see what happens in an extreme case of $\theta \rightarrow 90^{\circ}$, although it is somewhat unrealistic.

Table-1 Experimental conditions for "Series-V": experimental runs for velocity measurements.

Case No.	R/λ	θ(deg)	d/R	h (cm)	d (cm)	λ (cm)	Q (l/sec)	I ($\times 10^{-3}$)	Re($\times 10^{3}$)	Fr
V-1	0.0243	45	0.779	6.50	2.80	148	4.40	1.25	7.59	0.313
V-2		75					4.38	1.00	7.54	0.311
V-3		90					4.38	1.18	7.55	0.311
V-4	0.0152	45				236	4.19	1.18	7.23	0.299
V-5	0.0243		0.501	5.70	1.80	148	4.27	0.67	7.38	0.308

Table-2 Experimental conditions for "Series-S and R": experimental runs for flow resistance measurements.

(a) "Series-S": a channel with smooth perimeters made of plastic walls. "S-3" is a referring case. The hydraulic radius R is fixed to be R=2.5cm in all cases. In the hatched case numbers, a water surface profile is also measured.

Case No.	R/λ	θ(deg)	d/R	h (cm)	d (cm)	λ (cm)	Q (l/sec)	I ($\times 10^{-3}$)	Re ($\times 10^{3}$)	Fr
S-1	0	———	0.212	3.00	0.50	∞	2.11～8.29	0.50～5.0	4.18～16.2	0.348～1.35
S-2	0.0118	45	0.212	3.00	0.50	200	1.73～10.8	0.50～10.0	3.37～20.8	0.280～1.73
S-3	0.0159					148	1.80～8.44	0.50～6.7	3.50～16.3	0.291～1.36
S-4	0.0181					130	1.85～7.12	0.50～5.0	3.62～13.8	0.302～1.15
S-5	0.0226					104	2.16～11.1	0.67～14.0	4.17～21.8	0.347～1.81
S-6	0.0274					86	1.73～8.41	0.50～8.0	3.38～16.5	0.282～1.37
S-7	0.0159	30				148	2.01～7.84	0.50～5.7	3.99～15.6	0.333～1.30
S-8		60					1.77～6.64	0.52～5.0	3.41～13.1	0.284～1.09
S-9		75					1.76～6.38	0.50～4.4	3.42～12.5	0.286～1.04
S-10		90					1.93～7.05	0.50～5.0	3.79～14.0	0.316～1.17
S-11		45	0.765	3.96	1.80		2.50～6.18	1.4～6.5	4.73～11.7	0.386～0.955
S-12			1.19	4.71	2.80		2.39～5.72	1.7～8.1	4.40～10.5	0.355～0.848

(b) "Series-R": a channel with rough perimeters made of sand-paved walls. "S-3" is a referring case. The conditions are fixed to be d=1.48cm and I=1/400 in all cases.

Case No.	d/λ	θ(deg)	λ (cm)	Q (l/sec)	h (cm)	Re ($\times 10^{3}$)	Fr
R-1	0.0172	45	86	0.69～7.69	2.55～6.11	1.38～13.4	0.265～0.531
R-2	0.0142		104	0.85～7.99	2.68～6.18	1.68～13.9	0.289～0.541
R-3	0.00998		148	1.70～7.69	3.15～5.76	3.31～13.6	0.405～0.586
R-4	0.00616		240	1.28～8.91	3.10～5.59	2.50～15.9	0.314～0.714
R-5	0.00998	30	148	2.08～8.83	3.31～5.95	4.03～15.5	0.446～0.638
R-6		60		1.98～8.75	3.38～6.12	3.82～15.3	0.406～0.603
R-7	0	———	∞	0.96～9.56	1.96～5.74	1.70～14.4	0.624～0.743

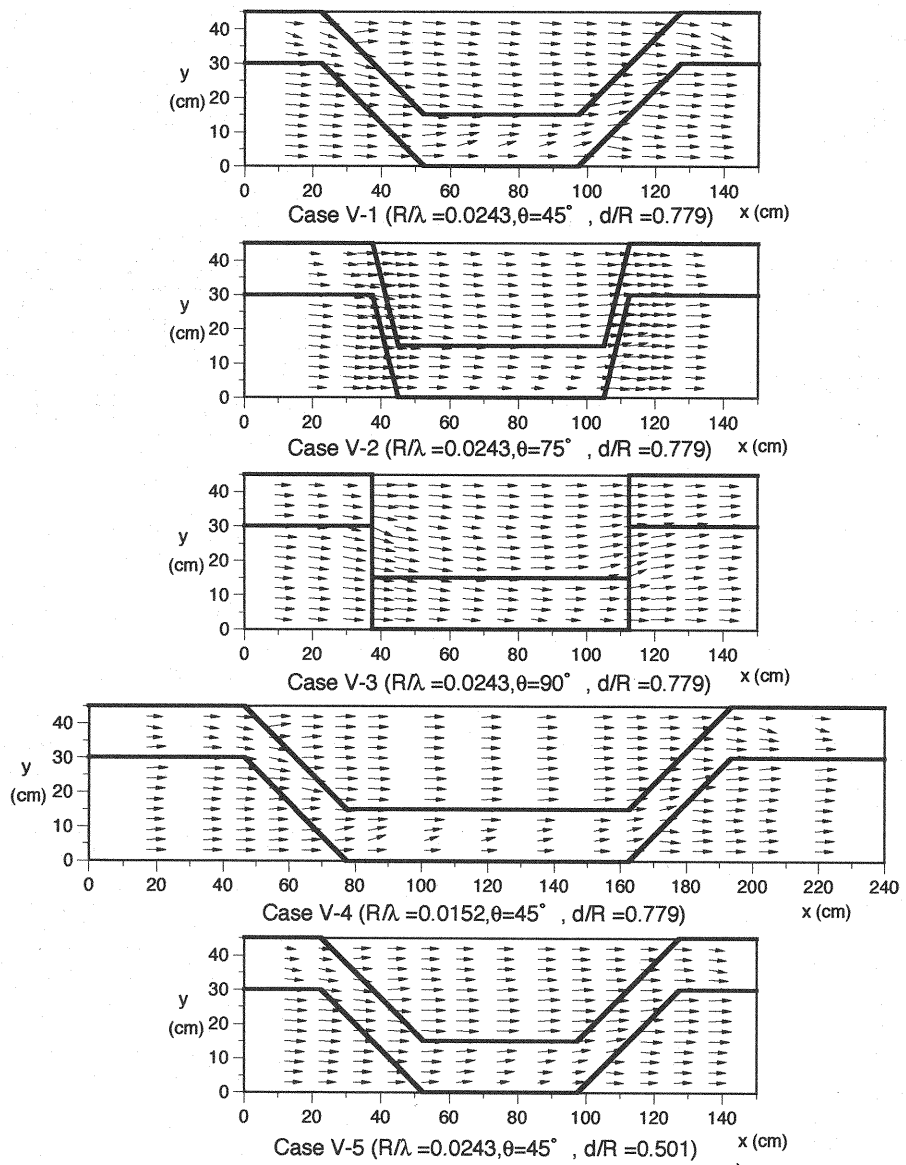

Fig.2 Velocity vectors in a horizontal plane of z=3.8cm for different profiles of channel geometry, "Series-V".

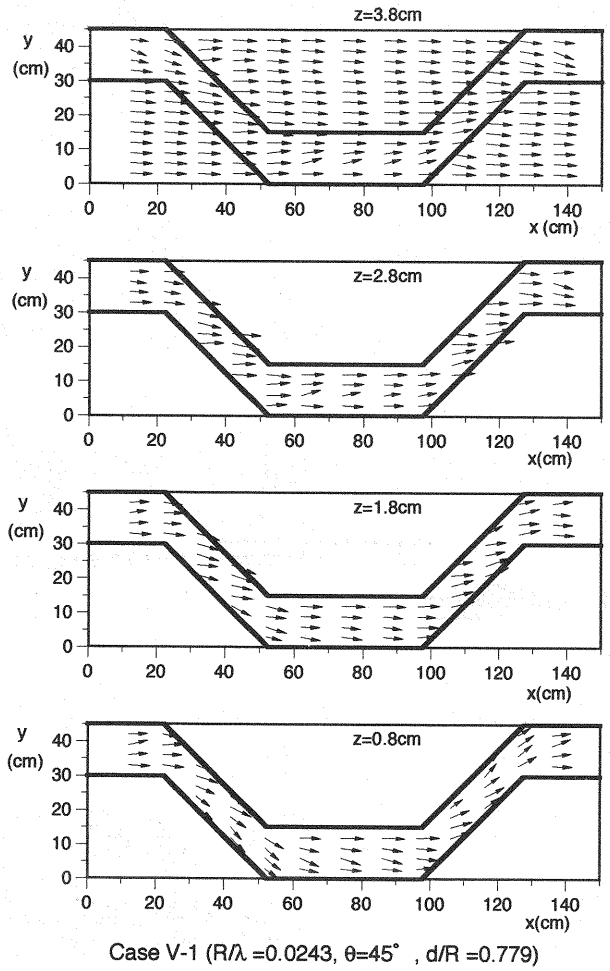

Fig.3 Velocity vectors in horizontal planes of different height, "Case V-1".

For θ=45° the flow field is significantly affected by the bed profile; the streamline is well directed along the main channel.

For θ=75° , however, flow tends to run straight independently on the main channel direction. Because velocity magnitude and direction are quite different between the upper and lower layers, drag force in this case must be more significant than that in smaller θ.

Effect of a longitudinal interval of a riffle structure, λ, is investigated through comparison between the cases V-1 and V-4. Local velocity fields around a diagonal edge of a riffle element are quite similar each other. But the streamline in V-4 runs more straightway in the middle of shallow region than in V-1. The reason is that the main channel has longer straight stretch in V-4, which helps flow to develop with being scarcely interrupted by the main channel's meander.

Comparison between V-1 and V-5 shows effect of riffles' height d on velocity fields. Streamlines in V-5 are straighter than V-1, because d in V-5 is lower than that in V-1 and it has less influence upon flow fields.

Velocity vectors in different depths are shown in Fig.3. Closer to the bed, more the streamlines tend to meander along the main channel. Closer

to the water surface, on the other hand, the flow runs more straightway. The velocity measurements suggest that strong interaction and shear stress exist between the upper and lower layers. This should be taken into consideration in theoretical modeling of flow dynamics.

Water Surface Profiles

A point-gauge measurement provides time-average of water surface profiles. Displacement from a mean water level, ΔH, is drawn in gray patterns in Figs.4 and 5. A darker pattern means higher water level.

Fig.4 shows water surface profiles for R/λ=0.0274, 0.0226 and 0.0159. It is seen that steady standing waves are generated through interaction between channel's bed and flow. Water surface displacement is significant along a diagonal edge of the main channel, where the flow is much interfered by the bed geometrical shape. Direction of the crest line is well correlated to the riffle-pool structure. Complicated surface profiles are observed around an intersection point between a straight side wall and a diagonal edge of the main channel, which are shown as "IP" in the figures. Magnitude of the water surface displacement could measure potential energy converted from flow kinetic energy. In other words, the water surface roughness is a measure of geometrical shape loss caused by the riffle-pool structure or a measure of the drag force. The displacement magnitude in each case is in the same order in Fig.4, which suggests that the energy conversion to the potential energy is approximately independent on the parameter R/λ. In other words, loss of flow

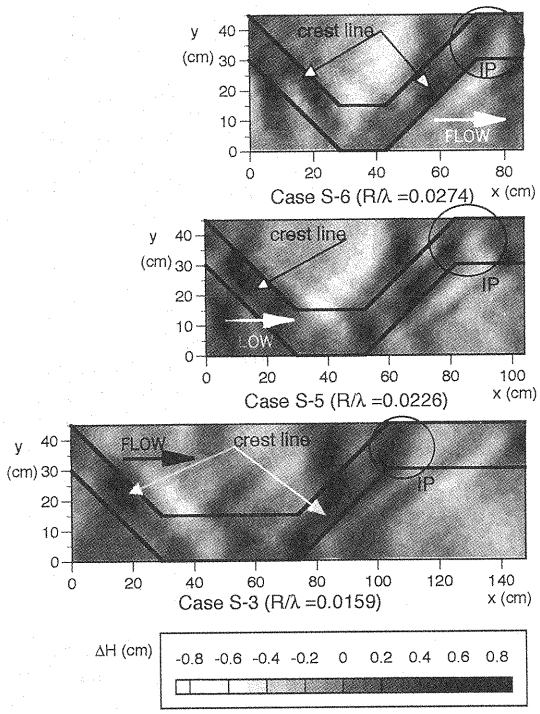

Fig.4 Water surface profiles for different R/λ, where an acute angle is fixed to be θ=45° .

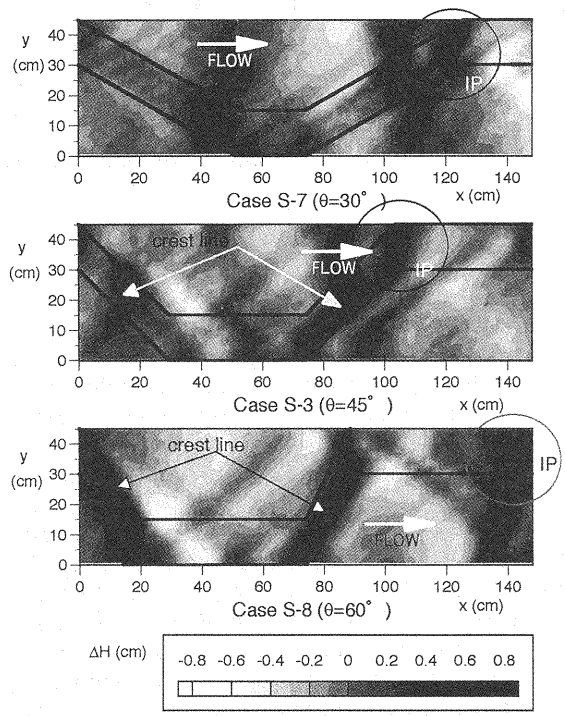

Fig.5 Changes in water surface profile with the acute angle θ, where a relative hydraulic radius is fixed to be R/λ=0.0159.

kinetic energy or drag force is not so much influenced by R/λ.

Dependency of water surface profiles on θ is shown in Fig.5. Water surface becomes rougher with increasing θ. This means that the more flow kinetic energy is converted into potential energy for the larger angle θ.

Since the water surface displacement must have a certain correlation with geometrical shape loss, examination of water surface profiles should help us in understanding and modeling of flow drag force. A more quantitative discussion will be made in a subsequent section regarding a drag force parameterization.

EVALUATION OF FLOW RESISTANCE

It is considered that flow resistance is composed of two factors; (1) friction force from wall shear stress and (2) drag force due to a riffle-pool structure. It is assumed in the following sections that the total flow resistance is given by a linear superposition of the two components. Therefore, what we need to do first is to evaluate the two components of resistance force separately as functions of hydraulic parameters. Second, they are integrated into the momentum equation in order to describe the total flow resistance.

Wall Shear Stress

Wall shear stress is investigated from momentum balance in a straight channel, because drag force is absent there. Two cases of compound cross section are considered; a totally smooth-walled channel and a channel with sand-pavement on its flood plain. In the latter case, an equivalent roughness height is measured to be k_S=2.77mm.

Friction coefficient for the plastic wall f_0 is well approximated by the Blasius's law (discussed later in Fig.7). Friction coefficient for the sand-pavement f_R is described by the following equation.

$$\sqrt{\frac{1}{f_R}} = 2.10 + 2.03 \log\left(\frac{175}{\mathrm{Re}\sqrt{f_R}} + \frac{k_S}{h}\right) \qquad (3)$$

This is well correlated to the experimental data as shown in Fig.6. The corresponding Manning's coefficient is identified to be n=0.0156.

Drag Force due to Riffle-Pool Structure

The "Series-S" dataset is introduced to empirically formulate the geometrical shape losses from the riffle-pool system. In this series the total flow force consists of wall shear on the smooth-walled perimeter and drag force due to the riffle-pool installment. The first component is evaluated from the straight-channel experiment discussed above. Then, it is subtracted from the total flow force to obtain the second component or the drag force.

First, the total flow force is described in terms of a friction coefficient f which is experimentally

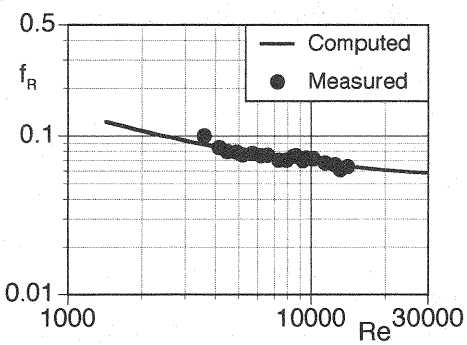

Fig.6 Friction coefficient as a function of Reynolds number Re in a rough-surface channel. The experimental data are compared with a theoretical curve given by Eq.(3).

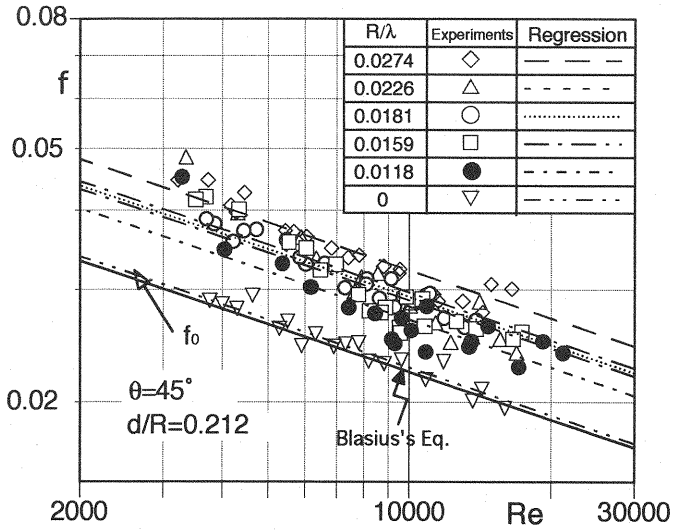

Fig.7 Functional dependencies of friction coefficient f on Re and R/λ for "Series-S".

formulated as in Eq.(2). Fig.7 is an example of this relationship obtained from the experiment, which is shown as a function of Re and R/λ. For every R/λ, f can be written by a Blasius-type formula as

$$f=K\cdot \mathrm{Re}^{-1/4} \tag{4}$$

A similar relationship was confirmed in plotting f with respect to θ and d/R.

The data from the straight-channel experiment (R/λ=0, Case S-1) are well approximated by the Blasius' law. Deviation of each line in Fig.7 from the straight-channel's data, i.e. $(f-f_0)$, corresponds to the drag force due to the channel bed geometry.

Now, the drag force is described by a drag coefficient C_D as $\rho C_D U^2/2$. Then, a one-dimensional momentum balance for every half streamwise distance of a riffle element, i.e. $\lambda/2$, can be written as follows.

$$\frac{\rho}{2}g\lambda AI-\frac{1}{2}(B+2h)\lambda\tau_0-\frac{\rho}{2}C_D U^2 A_d=0 \tag{5}$$

The first term is a gravity force, the second one a wall shear stress and the last one a drag force acting on a riffle element, respectively. Here, the cross-sectional areas on which the drag force acts is considered to be $A_d=(B-b)\,d$ (see Fig.1).

C_D is computed as follows.

First, a relation $\tau_0=f_0\rho U^2/8$ is substituted into τ_0 in the second term of Eq.(5). Here, f_0 is a friction coefficient for a smooth-walled straight channel, which is given by $f_0=K_0\mathrm{Re}^{-1/4}$ in Fig.7. Second, U in the second term of Eq.(5) is defined in terms of the friction coefficient f as $U=\sqrt{8gRI/f}$. Substituting them into Eq.(5), it is written as

$$g\lambda AI-\frac{f_0}{f}gRI(B+2h)\lambda-C_D U^2 A_d=0 \tag{6}$$

Since both of f and f_0 are inversely proportional to $\mathrm{Re}^{-1/4}$ as shown in Fig.7,

their fraction $f/f_0=K/K_0$ is independent on Re. Therefore, the third term of Eq.(6) or the drag force is expected to be dependent on Reynolds number as well. Giving a measured value of $U=Q/A$ and other channel's dimensions, C_D can be computed from Eq.(5). It is confirmed in plotting C_D and Re that C_D takes a constant value independently on Re as discussed above. An ensemble average of C_D in the plotting was employed.

In parameterization of C_D, the case S-3 is taken to be a referring case; quantities from the other cases are normalized by those of S-3. Here, $R/\lambda=0.0159$, $\theta=45^\circ$, $d/R=0.212$ for S-3. Its drag coefficient is denoted to be C_{DS}.

Relationships between C_D/C_{DS} and $(R/\lambda,\ \theta,\ d/R)$ are obtained from the experiment as in Figs.8, 9 and 10. Their regression relationships are

$$\frac{C_D}{C_{DS}}\left(\frac{R}{\lambda}\right)\equiv F\left(\frac{R}{\lambda}\right)=0.904 \qquad (7)$$

$$\frac{C_D}{C_{DS}}(\theta)\equiv G(\theta)=-\frac{1.83}{10^5}\theta^3+\frac{2.41}{10^3}\theta^2-\frac{6.94}{10^2}\theta+0.958 \qquad (8)$$

$$\frac{C_D}{C_{DS}}\left(\frac{d}{R}\right)\equiv H\left(\frac{d}{R}\right)=0.161\left(\frac{d}{R}\right)^2+0.0563\left(\frac{d}{R}\right)+0.981 \qquad (9)$$

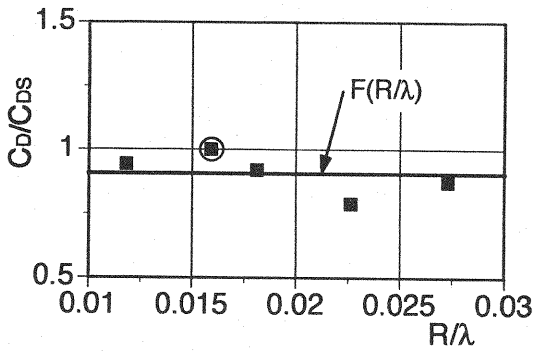

Fig.8 Experimental plotting of normalized drag coefficient C_D/C_{DS} as a function of R/λ.

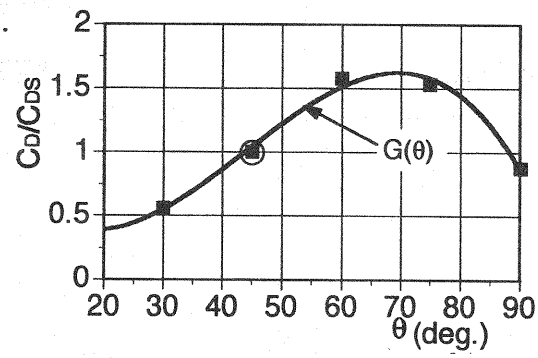

Fig.9 C_D/C_{DS} versus θ.

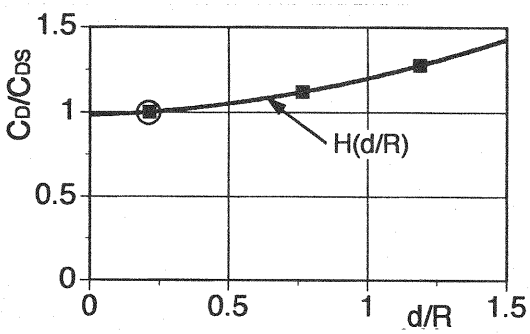

Fig.10 C_D/C_{DS} versus d/R.

It is shown in Figs.8 and 9 that the drag force stays constant independently on R/λ, while it increases with θ in the range of $\theta<60^\circ$. The dependency of C_D/C_{DS} on these two parameters is analogous to that observed in the water surface profiles of Figs.4 and 5; Fig.4 shows that water surface roughness does not change so much with varying R/λ, while it increases with θ in Fig.5. As discussed above, the water surface displacement reflects potential energy converted from kinetic energy of the channel flow And the drag force from the riffle-pool structure plays as the main driving force in this energy conversion process. In other words, the water surface roughness is a measure of the geometrical shape losses. From these discussions it is confirmed that the functional dependencies found in Figs.8 and 9 are consistent with the measurement of water surface profiles.

Eqs.(7), (8) and (9) are finally integrated into

$$\frac{C_D}{C_{DS}}\left(\frac{R}{\lambda},\theta,\frac{d}{R}\right)=F\left(\frac{R}{\lambda}\right)G(\theta)H\left(\frac{d}{R}\right) \tag{10}$$

FLOW RESISTANCE IN A CHANNEL COMPOSED OF SAND-PAVED RIFFLES AND SMOOTH-WALLED POOLS

By applying C_D obtained above, a momentum balance for this case is written by

$$\frac{\rho}{2}g\lambda AI-\frac{1}{2}(b+2h)\lambda\tau_0-\frac{1}{2}(B-b)\lambda\tau_R-\frac{\rho}{2}C_D U^2 A_d=0 \tag{11}$$

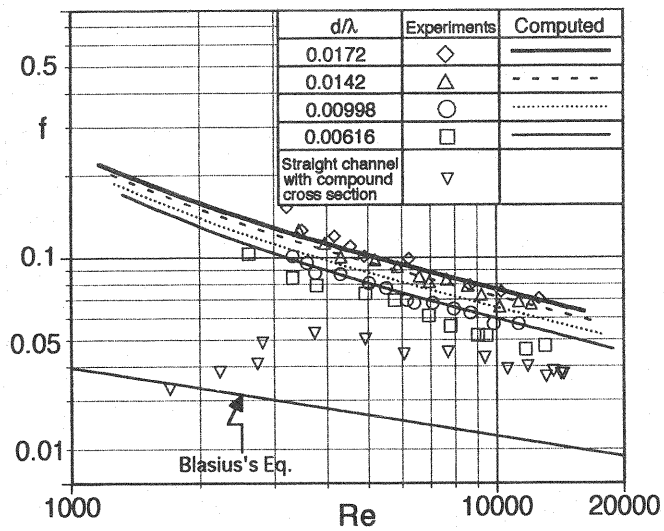

Fig.11 Functional dependencies of friction coefficient f on Re and d/λ. The model prediction is compared with the experimental data from "Series-R".

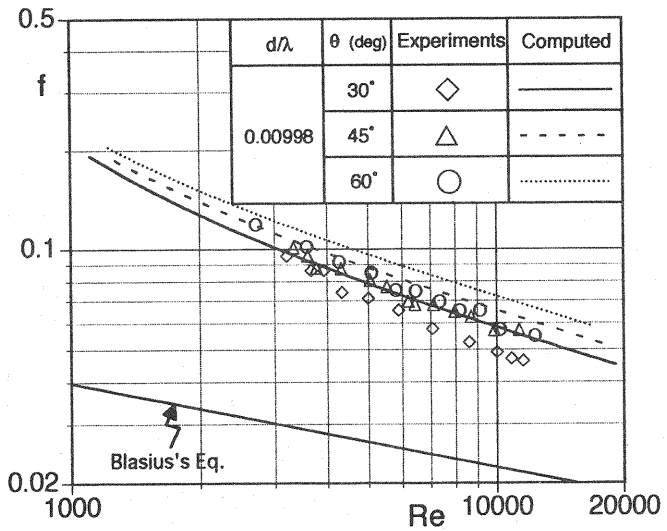

Fig.12 Functional dependencies of f on Re and θ. The notation is same to Fig.11.

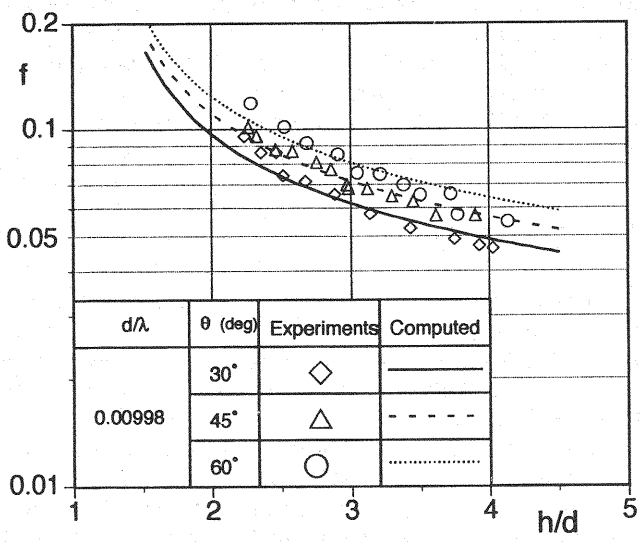

Fig.13 Functional dependencies of f on h/d and θ. The notation is same to Fig.11.

In Eq.(11) shear stress acting on the sand-paved riffle element τ_R is described by $\tau_R=\rho f_R U^2/8$, where f_R is already formulated in Eq.(3). The shear stress for the smooth-walled perimeter τ_0 and the drag coefficient C_D are respectively evaluated as before. After all, Eq.(11) can be solved with respect to U. The corresponding friction coefficient f is then computed.

The friction coefficient obtained in this way is shown as a function of parameters, (d/λ, θ, h/d) and Re in Figs.11 to 13. Here, the experimental data are compared with. The agreement between the computation and the measurement is fairy satisfactory. The analysis could be improved if internal shear between the main channel and the riffle are more directly taken into consideration.

CONCLUDING REMARKS

Velocity vectors, water surface profiles and flow resistance are experimentally investigated in open channels with various types of riffle-pool systems installed. The system is very simple and the result does not represent all the situations that could exist in river channels. In this study, however, focus is rather placed on a fundamental situation in which velocity, water depth and bed roughness varies in a channel course. The authors believe that the present system might not be so far from a prototype river system, since basic ideas in recent river restoration are to create variety in flow fields. However, more consideration should be taken, because the experimental conditions here are limited to low Reynolds numbers. A flow resistance analysis in terms of Manning's coefficient is necessary for practical use. Three-dimensional flow structures and evaluation of local flow force must be investigated more for improving the flow resistance analysis as well.

REFERENCES

1. Ervine,D.A. et al.: Factors affecting conveyance in meandering compound flows, J. Hydraulic Engineering, Vo.119, pp.1383-1399, 1993.

2. Fukuoka,S. and Fujita,K.: Prediction of flow resistance in compound channels and its application to design of river courses, Proc. Japan Soc. Civil Eng., No.411/II-12, pp.63-72, 1989 (in Japanese).
3. Fukuoka,S., Ohgushi,H., Kamura,D. and Hirao,S.: Hydraulic characteristics of the flood flow in a compound meandering channel, Proc. Japan Soc. Civil Eng., No.579/II-41, pp.83-92, 1997(in Japanese).
4. Fukuoka,S. and Watanabe,A.: Three dimensional analysis on flows in meandering compound channels, Proc. Japan Soc. Civil Eng., No.586/II -42, pp.39-50, 1998 (in Japanese).
5. Ida,T.: Steady flow in a wide open channel, Effects of cross-section geometry on its flow characteristics, Proc. Japan Soc. Civil Eng., No.69 (3-2), 1960 (in Japanese).
6. Ishigaki,T., Muto,Y., Takeo,N. and Imamoto,H.: Fluid mixing and boundary shear stress in compound meandering channel, Proc. 27th Conf. IAHR, theme-A, pp.763-768, 1997.
7. James,C.S. and Wark,J.B.: Conveyance estimation for meandering channels, Report SR 329, Hydraulic Res., Wallingford, 1992.
8. Jin,H., Egashira,S. and Liu,B.: Characteristics of meandering compound channel flow evaluated with two-layered 2-D method, Annual J. Hydraulic Engineering, JSCE, Vol.40, pp.717-724, 1996.
9. Rameshwaren,P. and Willetts,B.B.: The mixing mechanism in turbulent two-stage meandering channel flows, Proc. 27th Conf. IAHR, theme-A, pp.746-751, 1997.
10. Rahman,M.M., Nagata,N., Hosoda,T. and Muramoto,Y.: Experimental study on morphological process of meandering channels with bank erosion, Annual J. Hydraulic Engineering, JSCE, Vol.40, pp.947-952, 1996.
11. Utami,T. and Ueno,T.: Flood flow and sediment transport in meandering channel with compound corss-section, Annual J. Hydraulic Engineering, JSCE, Vol.40, pp.933-940, 1996 (in Japanese).
12. Whiting,P.J. and Deitrich,W.E.: Experimental constraints on bar migration through bends: Implications for meander wave length selection, Water Resources Res., Vol.29(4), pp.1091-1101, 1993.

APPENDIX-NOTATION

A_d = cross sectional area of a riffle element, defined by $A_d=(B-b)\,d$;
b = width of a pool or a main channel;
b' = riffle element's width;
B = width of open channel;
C_D = Drag coefficient;
C_{DS} = Drag coefficient for a referring case;
d = riffle element's height;
D = hydraulic depth;
f = friction coefficient defined by $f\equiv 8gRI/U^2$;
f_R = friction coefficient for a sand-paved channel;
f_0 = friction coefficient for a smooth-walled channel;
Fr = Froude number defined by $\mathrm{Fr}\equiv U/\sqrt{gD}$;
g = gravity acceleration;
h = water depth;
I = channel bed slope;
k_S = equivalent roughness height of sand pavement;
K = a proportional coefficient of a friction power law;
K_0 = a proportional coefficient of a friction power law in a smooth-walled straight channel;

R = hydraulic radius;
Re = Reynolds number defined by $\mathrm{Re} \equiv UR/\nu$;
U = cross-sectional average of streamwise mean velocity;
λ = streamwise interval of a riffle-pool system;
θ = acute angle between the diagonal wall of a trapezoidal riffle element and the streamwise direction;
τ = wall shear stress;
τ_0 = wall shear stress for a smooth-walled channel;
τ_R = wall shear stress for a channel with sand-pavement.

(Received September 29, 1998 ; revised March 5, 1999)